Representing inhibition in growth kinetics: the Haldane KIS

Nan Pan[a], Liu-Di Lu[b], Olivier Bernard[c,d]

[a] *LIX, CNRS UMR 7161, École Polytechnique, Institut Polytechnique de Paris, 1 rue Honoré d'Estienne d'Orves, 91120 Palaiseau, France*

[b] *Section of Mathematics, University of Geneva, rue du Conseil-Général 5-7, CP 64, 1205, Geneva, Switzerland*

[c] *INRIA Centre d'Université Côte d'Azur, BIOCORE Project-Team, Université Nice Côte d'Azur, 2004, Route des Lucioles - BP 93, 06902 Sophia-Antipolis Cedex, France*

[d] *Sorbonne Université, CNRS, Laboratoire d'Océanographie de Villefranche, 181 Chemin du Lazaret, 06230 Villefranche-sur-mer, France*

Abstract

This article focuses on the practical application of the Haldane model in studying microbial growth, a critical aspect in various industrial and environmental contexts. We examined four existing descriptions of the Haldane model in the literature, and introduced an additional description based on only two parameters. We investigated the interrelations among these five descriptions in the context of photoinhibited microalgae growth rate. Using state-of-the-art model identification technique, we carried out sensitivity analyses on each parameter across all descriptions. Furthermore, we introduced a novel criterion to account for the model accuracy in the selection of the most suitable description.

Using experimental data from literature on response to irradiance, we determined the parameter values for each description and for each data set. The correlation between each parameter is discussed. When parameters within a description exhibit strong correlations, they convey similar information, rendering the description less efficient. The sensitivity analysis, combined with an upgrade of the Akaike information criterion ($\mathrm{AIC_c}$) and Bayesian information criterion (BIC), identified our two-parameter description as the optimal choice for representing microalgae growth rate in response to irradiance variations. Importantly, the novel information criterion, namely PEMAC, outperforms traditional criteria such as $\mathrm{AIC_c}$ and BIC in distinguishing between equivalent descriptions. This work illustrates the hidden complexity in inhibition models and end up with a wise recommendation for the modelling of inhibition: "Keep It Simple (KIS)".

Keywords: Haldane model, microalgae, parameter identification, sensitivity analysis, AIC, BIC

1. Introduction

Microorganisms, such as bacteria, cyanobacteria, microalgae or yeasts have tremendous potential for a wide range of applications. Due to their small size and simple cellular structure, they can be grown quickly and efficiently in bioreactors, requiring minimal resources. Depending on the species, these tiny organisms can be grown for pollution removal, feed or food production thanks to their protein content, and for the production of high value-added products in the chemical industry [1, 2, 3]. Additionally, microorganisms offer avenues for biofuel production, using their potential to store lipids and carbohydrate that can be converted into biodiesel and ethanol [4, 5]. The photosynthetic microorganisms (cyanobacteria and microalgae) can even contribute to fix CO_2 and to transform it into valuable products for green chemistry or for biofuel production [6].

Modelling bioreactors is the cornerstone for their efficient supervision, control and optimization [7]. There exists a broad range of mathematical models which can represent the growth of microorganisms as

Email addresses: pan@lix.polytechnique.fr (Nan Pan), liudi.lu@unige.ch (Liu-Di Lu), olivier.bernard@inria.fr (Olivier Bernard)

a function of the main factors affecting their metabolism. The most famous kinetics model is probably the Monod model [8], particularly for representing substrate-limited microorganism growth. Here, we focus on a class of phenomena which appear when there is an excess in one of the factor inhibiting growth. For instance, the Aiba growth inhibition model correlates reduced specific growth rate with elevated product concentration [9], while the Edward model elucidates the protective effect of diffusional limitation at high substrate concentrations [10]. We also refer to [11] for a brief review of some other widely used models. The Haldane model [12] is one of the most used model in biology to represent enhancement at low dose and then inhibition for high dose [13, 14, 15, 16]. It finds numerous applications for substrates which can become inhibiting, such as phenol, ethanol or volatile fatty acids [17, 18]. In another class of applications, the Haldane model is used to represent the excess of light on photosynthetic microorganisms [15, 19] triggering photoinhibition. Nonetheless, practical application of the Haldane model often proves intricate due to varying descriptions associated with different parameterization sets. In mathematical terms, it can be defined as the ratio of a term proportional to the substrate concentration (or the light intensity) and a second order polynomial. In other terms, the inverse of the yield (ratio of the factor to the growth rate) is a polynomial of second order. There exists numerous parameterizations of this model, and the objective of this paper is to assess their consequences in terms of the efficiency of the parameter identification process and of the resulting model accuracy.

According to the context, different descriptions of the Haldane model exist in the literature. In 1965, J.B.S. Haldane [12] uses three parameters which were (wrongly) defined as $\bar{\mu}$ the maximum specific growth rate (h^{-1}), K_x the half-velocity concentration (mg L^{-1}), and K_i the inhibition coefficient(mg L^{-1}). In subsequent studies, J.F. Andrews [20] uses the same notation for another three parameters, $\bar{\mu}$ the maximum specific growth rate in the absence of inhibition (s^{-1}), K_x the lowest concentration of substrate at which the specific growth rate is equal to one-half the maximum specific growth rate in the absence of inhibition (mg L^{-1}), and K_i the highest substrate concentration at which the specific growth rate is equal to one-half the maximum specific growth rate in the absence of inhibition (mg L^{-1}). J.C.H Peeters et al. [21] rather use three arbitrary parameters a, b, and c, which are later determined through real measurements. Bernard et al. [15] present a new description for the influence of light on phytoplankton growth rate. This description also contains three parameters, with $\mu_{\max}$ the maximum growth rate for the optimal irradiance (s^{-1}), α the initial slope of the light response curve ($\mu\mathrm{mol}^{-1}$ photons m^2), and x_{opt} the value of substrate or irradiance for which the growth is maximal (μmol photons $\mathrm{m}^{-2}\,\mathrm{s}^{-1}$). The above four descriptions are summarized in the following equations:

$$\mu^1(x) = \frac{\mu_{\max} x}{x + \frac{\mu_{\max}}{\alpha}(\frac{x}{x_{\mathrm{opt}}} - 1)^2}, \tag{1}$$

$$\mu^2(x) = \frac{\bar{\mu} x}{x + K_x + \frac{x^2}{K_i}}, \tag{2}$$

$$\mu^3(x) = \frac{x}{ax^2 + bx + c}, \tag{3}$$

$$\mu^4(x) = \bar{\mu}\frac{x}{x + K_x}\frac{K_i}{x + K_i}. \tag{4}$$

In this article, we introduce a new Haldane type description for characterizing the growth

$$\mu^5(x) = 4\gamma_{\max}\frac{xx^\star}{(x + x^\star)^2}, \tag{5}$$

which requires only two parameters denoted by $\gamma_{\max}$ and $x^\star$, and will be further discussed.

In this paper, the objective is to compare the performance of the existing descriptions (1)-(4) in the idea to highlight the most accurate description. We also compare them with the new description (5). To compare different descriptions, we evaluate their performance in data sets representing photoinhibition for various microalgae growth experiments. These data sets are used to determine the optimal parameters by fitting them to experimental data. We use standard identification methods to find the best description for the experimental data by minimizing a loss function representing the model error. Although the descriptions (1)-(5) are all mathematically equivalent, some provide better performance than the others in specific situations, meaning that the identification point of view will change the accuracy of the description. The results of identification thus reveal fundamental differences between these descriptions.

There are several criteria for assessing the performance of a model for a given dataset, such as Akaike's information criterion (AIC) [22, 23, 24] and Bayesian information criterion (BIC) [25, 26]. They are used for model selection in the analysis of empirical data accounting for the differences in the model degrees of freedom. By comparing the values of AIC, BIC and the results of identification, we can determine the best model. However, these criteria become less efficient when it comes to distinguish equivalent descriptions of one model. For this reason, we introduce a new criterion based on the criteria AIC and BIC to improve the sensitivity for evaluating various descriptions of one model.

The current study is organized as follows. After providing the relation between various descriptions in Section 2, we introduce the data sources and methods for the analysis. Section 3 presents some numerical results with detailed discussion. We conclude in Section 4 with some comments and remarks on the findings of the study.

2. Materials and methods

2.1. Objectives

Our main objective is to fit the experimental data using the five descriptions (1)-(5) and to determine the most appropriate parameter values for each description. We assess the uncertainty associated with the description predictions and identify the optimal parameterization for the given experimental conditions. To this end, we consider eight different microalgae species on the light response to test the five descriptions under different conditions and evaluate the best formulations.

2.1.1. Growth response with Skeletonema costatum [27]

Anning et al. [27] study the growth of the diatom *Skeletonema costatum* strain CCMP 1332 (Plymouth Culture Collection). The algae cells are cultured under the same conditions, except for the irradiance levels. Here, we focus on the curve obtained for the pre-acclimation at $1200\,\mu\mathrm{mol\,photons\,m^{-2}\,s^{-1}}$, for which the photoinhibition is more marked. Labelled $NaH^{14}CO_3$ was used to culture the algal cells simultaneously over a gradient of irradiances to determine the photosynthetic carbon fixation.

2.1.2. Growth response via oxymetry for seven species of phytoplankton [28]

Yang et al. [28] investigate the photosynthetic response of seven strains of phytoplankton, comprising three strains of marine phytoplankton (*Isochrysis galbana*, *Dunaliella salina*, and *Platymonus subcordiformis*) and four strains of freshwater phytoplankton (*Chlorococcum sp.* FACHB-1556, *Microcystis aeruginosa* FACHB-905, *Microcystis wesenbergii* FACHB-1112, and *Scenedesmus obliquus* FACHB-116.). The cells are cultured at an irradiance of $60\,\mu\mathrm{mol\,photons\,m^{-2}\,s^{-1}}$ for 12 hours per day and at a temperature of $26 \pm 1°\mathrm{C}$ for 7 to 10 days. The cells are then subjected to increasing levels of irradiance, ranging from 0 to 1200 ($\mu\mathrm{mol\,photons\,m^{-2}\,s^{-1}}$), provided by a digital LED light source at a temperature of $25 \pm 1°\mathrm{C}$. The oxygen-evolving rate is measured using dissolved oxygen measurements.

2.2. Analysis

The parameters in description (1) have a biological meaning. Indeed, $\mu_{\max}$ is the maximum growth rate for the optimal irradiance x_{opt}, and α is the initial slope of the response curve. The growth kinetics for this description is represented in Figure 1 together with the three associated fundamental descriptors of the curve.

In the other descriptions, the parameters do not have a direct interpretation, but can be related to the three fundamental descriptors $\mu_{\max}$, x_{opt}, and α in the growth curve as follows:

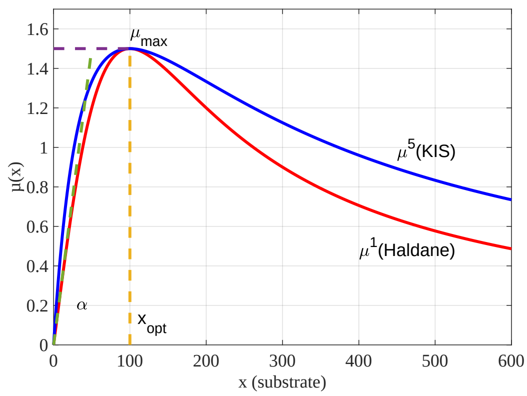

Figure 1: Representation of the Haldane model (description (1)), in red, parameterized with the three fundamental descriptors $\mu_{\max}$, the maximum growth rate for the optimal irradiance x_{opt} and α, the initial slope. The simplified KIS model (description (5)) is also represented in blue.

1. Description (2):

$$\bar{\mu} = \frac{\mu_{\max}\alpha x_{\text{opt}}}{\alpha x_{\text{opt}} - 2\mu_{\max}}, \quad K_x = \frac{\mu_{\max} x_{\text{opt}}}{\alpha x_{\text{opt}} - 2\mu_{\max}}, \quad K_i = \frac{x_{\text{opt}}(x_{\text{opt}}\alpha - 2\mu_{max})}{\mu_{\max}}, \tag{6}$$

   with the units of each parameter $\bar{\mu}$ (inverse of time), K_x and K_i (same as x). Note that the parameters of this model are all complex combinations of the fundamental descriptors.

2. Description (3):

$$a = \frac{1}{\alpha x_{\text{opt}}^2}, \quad b = \frac{1}{\mu_{\max}} - \frac{2}{\alpha x_{\text{opt}}}, \quad c = \frac{1}{\alpha}, \tag{7}$$

   with units for b (time), a (time per unit of x) and c (time times unit of x). We observe that the parameter c is directly connected with α, and the parameter a is deduced from α and x_{opt}. Parameter b results from the three fundamental descriptors.

3. Description (4):

$$\bar{\mu} = \alpha K_x, \quad K_x K_i = x_{\text{opt}}^2, \quad K_x + K_i = \frac{(\alpha x_{\text{opt}} - 2\mu_{\max})x_{\text{opt}}}{\mu_{\max}}, \tag{8}$$

   with the unit of $\bar{\mu}$ (inverse of time), K_x and K_i the same units as x. Note that here, there are two (equivalent) possible values for the couple (K_x, K_i), which illustrates the dramatic identifiability issue with this model [29].

4. Description (5):

$$\gamma_{\max} = \mu_{\max}, \quad x^\star = x_{\text{opt}}, \quad \frac{4\gamma_{\max}}{x^\star} = \alpha, \tag{9}$$

   with the units of $\gamma_{\max}$ in time inverse, and $x^\star$ the same unit as x. Parameter $x^\star$ corresponds to the value of x for which the growth rate is the maximum. Parameter $\gamma_{\max}$ is the maximum growth rate obtained for $x^\star$. Note that, even if these values are close, $\frac{\gamma_{\max}}{x^\star} \neq \alpha$ in Figure 1, which helps to distinguish the two curves. Remark also that there are only two parameters in this description.

Let us denote by θ^k the parameter set corresponded to the description μ^k in (1)-(5). More precisely, $\theta^1 := (\mu_{\max}, \alpha, x_{\text{opt}})$ for (1), $\theta^2 := (\bar{\mu}, K_x, K_i)$ for (2), $\theta^3 := (a, b, c)$ for (3), $\theta^4 := (\bar{\mu}, K_x, K_i)$ for (4), $\theta^5 := (\gamma_{\max}, x^\star)$ for (5). Let us denote by m the number of parameters and by θ_j^k, $j = 1, \ldots, m$ each element of the parameter set θ^k. For instance, in (1), $\theta_1^1 = \mu_{\max}$, $\theta_2^1 = \alpha$, and $\theta_3^1 = x_{\text{opt}}$. In particular, $m = 3$ for descriptions (1)-(4) and $m = 2$ for the description (5).

2.2.1. Parameter identification

For experimental data from Section 2.1.1 and Section 2.1.2, we identify the appropriate parameter set θ^k for each description μ^k. For each microalgae species, let us denote by $(x_i)_{i=1}^n$ the irradiance samples (with n the size of the samples) and $\mu_{\exp}(x_i)$ the associated experimental estimations of the growth rate. We denote by $\mu^k(x_i, \theta^k)$ the growth rate evaluated at the light sample x_i using the description μ^k. The sum of the squared error (SSE) [24, 30] is given by:

$$\text{SSE} := \sum_{i=1}^{n} (\mu_{\exp}(x_i) - \mu^k(x_i, \theta^k))^2. \tag{10}$$

For each description μ^k, the best parameter set θ^k is identified by minimizing the SSE value. We use the Nelder–Mead simplex algorithm [31] implemented in the *fminsearch* function of Matlab.

2.2.2. Sensitivity analysis

Once the best parameter set θ^k has been identified, we compute the sensitivity equations to determine the Fisher information matrix (FIM) for comparing different descriptions [32]. The FIM is defined by

$$F := (\frac{\partial \mu^k}{\partial \theta^k}(x))^T Q \frac{\partial \mu^k}{\partial \theta^k}(x), \tag{11}$$

where Q is a square matrix representing the inverse of the covariance matrix of the measurement error. This information was not provided for $\mu_{\exp}(x_i)$ in the considered experimental data. We therefore assumed a 10% standard variation for each measurement, except for the lowest values where this value is saturated at a minimum level, following the strategy of [33]. More formally, we assume that the standard variation vector is:

$$W := \max_{i=1,\ldots,n} \Big(0.1\mu_{\exp}(x_i), 0.02 \max_{i=1,\ldots,n} \big(\mu_{\exp}(x_i)\big)\Big). \tag{12}$$

We then define Q as a diagonal matrix with entries $Q_{ii} := 1/W_i^2$.

For each parameter set θ^k, the standard deviation is defined by

$$\sigma := s\sqrt{n\text{diag}(V)}, \tag{13}$$

where $V := F^{-1}$ is the covariance matrix of parameter estimation error, and s is the residual mean square with:

$$s^2 := \frac{\sum_{i=1}^{n} (\mu^k(x_i, \theta^k) - \mu_{\exp}(x_i))^T Q_i (\mu(x_i, \theta^k) - \mu_{\exp}(x_i))}{n - m}. \tag{14}$$

From the parameter standard deviation, we can compute the prediction interval (PI) by

$$PI := \mu^k \pm Ze, \tag{15}$$

where Z is the value of Student's t-distribution choosing a significance level 0.05, and e is the error propagation with $e := \sqrt{\sum_{j=1}^{m} (\frac{\partial \mu^k}{\partial \theta_j^k})^2 \sigma_j^2}$. The adequacy of the description μ^k to the experimental measurements is the first criterion to assess its performance.

Additionally, the sensitivity of the parameter θ_j^k is computed as the normalized sensitivity [34]

$$S_j := (\frac{\sigma_j}{e} \frac{\partial \mu^k}{\partial \theta_j^k})^2. \tag{16}$$

2.2.3. Description selection criteria

The Akaike's information criterion (AIC) [22, 23, 24] and the Bayesian information criterion (BIC) [25, 26] are often used to select and compare non-equivalent models. We recall here the definition of AIC

$$\mathrm{AIC} := n\log(\frac{\mathrm{SSE}}{n}) + 2(m+1). \tag{17}$$

For small-samples, when $\frac{n}{m+1} < 40$, the AIC becomes the corrected Akaike information criterion ($\mathrm{AIC_c}$), given by :

$$\mathrm{AIC_c} := \mathrm{AIC} + \frac{2(m+1)(m+2)}{n-m-2}. \tag{18}$$

The Bayesian information criterion is given by:

$$\mathrm{BIC} := n\log(\frac{\mathrm{SSE}}{n}) + (m+1)\log(n). \tag{19}$$

However, both criteria are less sensitive when comparing equivalent descriptions for a same model. Let us denote by $\bar{e}$ the average of the error propagation e, which is an important criterion for qualifying the model accuracy

$$\bar{e} := \frac{1}{n}\sum_{i=1}^{n}\sqrt{\sum_{j=1}^{m}(\frac{\partial\mu^k}{\partial\theta_j^k}(x_i))^2\sigma_j^2}. \tag{20}$$

Based on $\mathrm{AIC_c}$ and BIC criteria, we introduce a new criterion, namely PEMAC (Propagated Error Modified Akaike Criterion), to account for the model accuracy in the fit assessment. More precisely, this criterion is defined by

$$\mathrm{PEMAC} := \begin{cases} 2n\log(\bar{e}) + n\log(\frac{\mathrm{SSE}}{n}) & \\ \quad + (m+1)\log n, & \frac{n}{m+1} \geq 40, \\ 2n\log(\bar{e}) + n\log(\frac{\mathrm{SSE}}{n}) & \\ \quad + \frac{2(m+1)(m+2)}{n-m-2}, & \frac{n}{m+1} < 40. \end{cases}$$

We will then test and compare our criterion with $\mathrm{AIC_c}$ and BIC to select the best descriptions among (1)-(5).

3. Results and discussion

In this section, we present some numerical results related to the five descriptions (1)-(5). Our analyses are based on the experimental data for the light response of microalgae, for eight different microalgae species. For all of them, we identify the parameters, present the sensitivity and the performance of each description.

3.1. Parameter identification

For each description μ^k among (1)-(5), the optimal parameter set θ^k varies from different experimental conditions and different microalgae species. Table 1 presents the optimal parameter sets and the SSE values for each description and for eight microalgae species. The SSE values for the species *Skeletonema costatum* is smaller not only due to the quality of the fit, but also because the measurement method is different, and with different units. For the seven other species, the SSE values are in the scale of 10^{-5}, except for the descriptions (4) and (5) with the species *Microcystis wesenbergii* FACHB-1112, *Scenedesmus obliquus* FACHB-116 and *Chlorococcum sp.* FACHB-1556, where the SSE values are in the scale of 10^{-4}. This reveals that the three descriptions (1)-(3) under their identified parameter set fit slightly better the experimental data in [28] comparing with (4) and (5). Although the description (1) is designed to study the influence of the irradiance on phytoplankton growth rate, we observe that there is no much difference on the SSE values

		1	2	3	4	5	6	7	8
(1)	$\mu_{\max}$	3.8436×10^{-5}	0.0339	0.0373	0.0335	0.0254	0.0877	0.0624	0.0805
	α	9.0614×10^{-8}	1.0096×10^{-4}	2.6351×10^{-4}	7.4685×10^{-4}	3.3149×10^{-4}	4.9411×10^{-4}	3.9217×10^{-4}	3.5048×10^{-4}
	x_{opt}	965.1726	697.4415	439.1005	253.0296	342.5652	339.4417	319.9471	484.9611
SSE		1.1164×10^{-10}	1.2346×10^{-5}	1.0841×10^{-5}	4.6218×10^{-5}	1.0985×10^{-5}	6.0475×10^{-5}	3.5333×10^{-5}	3.1000×10^{-5}
(2)	$\bar{\mu}$	3.1756×10^{-4}	0.9330	0.1050	0.0518	0.0458	-1.9147	11.9335	1.5156
	K_x	3504.5484	9240.9056	398.3028	69.4167	138.2674	-3875.0132	30429.2456	4324.3801
	K_i	265.8140	52.6380	484.0769	922.3136	848.7246	-29.7342	3.3641	54.3864
SSE		1.1164×10^{-10}	1.2346×10^{-5}	1.0841×10^{-5}	4.6218×10^{-5}	1.0985×10^{-5}	6.0475×10^{-5}	3.5333×10^{-5}	3.1000×10^{-5}
(3)	a	11.8466	0.0204	0.0197	0.0209	0.0257	0.0176	0.0249	0.0121
	b	3148.9876	1.0718	9.5276	19.2887	21.8174	-0.5223	0.0838	0.6598
	c	1.1036×10^{7}	9904.8464	3794.8752	1338.9598	3016.6396	2023.8331	2549.9064	2853.2691
SSE		1.1164×10^{-10}	1.2346×10^{-5}	1.0841×10^{-5}	4.6218×10^{-5}	1.0985×10^{-5}	6.0475×10^{-5}	3.5333×10^{-5}	3.1000×10^{-5}
(4)	$\bar{\mu}$	1.5234×10^{-4}	0.1318	0.1449	0.0565	0.0576	0.3138	0.2241	0.2989
	K_x	1273.9800	914.5639	458.7265	75.6161	173.8978	343.2328	323.1022	544.4024
	K_i	1274.3248	914.5640	458.7265	846.6974	674.8267	343.2328	323.1022	544.4024
SSE		1.5685×10^{-10}	4.3482×10^{-5}	2.0970×10^{-5}	4.6218×10^{-5}	1.0985×10^{-5}	6.0296×10^{-4}	2.8402×10^{-4}	3.0619×10^{-4}
(5)	$\gamma_{\max}$	$3.8086\ 10^{-5}$	0.0329	0.0362	0.0351	0.0257	0.0784	0.0560	0.0747
	$x^{\star}$	1273.9800	914.5640	458.7265	248.7247	338.0766	343.2328	323.1022	544.4024
SSE		1.5685×10^{-10}	4.3482×10^{-5}	2.0970×10^{-5}	6.8655×10^{-5}	1.2139×10^{-5}	6.0296×10^{-4}	2.8402×10^{-4}	3.0619×10^{-4}

Table 1: Best estimates of five descriptions (1)-(5) for each microalgae species. (1: *Skeletonema costatum*, 2: *Isochrysis galbana*, 3: *Dunaliella salina*, 4: *Platymonus subcordiformis*, 5: *Chlorococcum sp.* FACHB-1556, 6: *Microcystis aeruginosa* FACHB-905, 7: *Microcystis wesenbergii* FACHB-1112, 8: *Scenedesmus obliquus* FACHB-116.)

between (1) and the other four descriptions (2)-(5). This is not surprising since the underlying mathematical model is identical (except for (5)), and only the way the parameters are expressed is changing. Moreover, we observe that, in general, the identified values of $\gamma_{\max}$ (resp. $x^{\star}$) in description (5) are quite similar to $\mu_{\max}$ (resp. x_{opt}) description (1). This further confirms the physical meaning of the two parameters in the proposed description (5). We will use the optimal parameter values in Table 1 for the tests.

3.2. Correlation matrix of parameter estimation error

Based on the covariance matrix of the parameter estimation error V, we compute the correlation matrix of the parameter estimation error, and illustrate in Table 2 for all five descriptions and eight microalgae species. We consider that two parameters θ_i^k and θ_j^k are correlated if the absolute value of their correlation exceeds 0.9. Under this consideration, we observe that the three parameters in the description (1) are rather uncorrelated to each other, as well as the two parameters in the description (5). On the other hand, all three parameters in the description (2) are strongly correlated. There are only two microalgae species for which we are able to determine the correlation matrix for (4). This is due to the fact that the related Fisher information matrix F is singular. For these two species, we observe once again a strong correlation between the three parameters in the description (4). Regarding the description (3), there is a strong correlation between the parameters a and b, and both are rather uncorrelated with the parameter c. The correlation coefficient between parameters assesses whether the parameters are independent. If one of the parameters is not independent, then the correlated parameters are likely to produce similar information, and the description is thus less efficient. Based on our observations, the descriptions (1) and (5) are more suitable for representing the growth rate with respect to the irradiance for the eight microalgae species.

3.3. Best description of the inhibition kinetics

In general, the minimum value of AIC_c or BIC reveals the best trade-off between the number of parameters m and the data fit ability among different models. However, this becomes less clear for selecting equivalent descriptions of one model. Table 3.3 presents the AIC_c, BIC and PEMAC values of all five descriptions (1)-(5) for each microalgae species. We observe that the values of AIC_c and BIC do not vary significantly among the five descriptions, especially for the species *Platymonus subcordiformis* and *Chlorococcum sp.* FACHB-1556. Thus, based on the values of AIC_c and BIC, it is less clear which description is better among (1)-(5). This ambiguity disappears when considering the criterion PEMAC. Indeed, there is a clear difference of the PEMAC value between the five descriptions, even in the case of the species

	1			2			3			4			5			6			7			8		
(1)	$\mu_{\max}$	α	x_{opt}	$\mu_{\max}$	α	x_{opt}	$\mu_{\max}$	α	x_{opt}	$\mu_{\max}$	α	x_{opt}	$\mu_{\max}$	α	x_{opt}	$\mu_{\max}$	α	x_{opt}	$\mu_{\max}$	α	x_{opt}	$\mu_{\max}$	α	x_{opt}
$\mu_{\max}$	1.00	-0.30	0.05	1.00	-0.39	-0.07	1.00	-0.47	-0.32	1.00	-0.46	-0.38	1.00	-0.47	-0.39	1.00	-0.50	-0.19	1.00	-0.46	-0.24	1.00	-0.51	-0.30
α	-0.30	1.00	0.53	-0.39	1.00	0.47	-0.47	1.00	0.18	-0.46	1.00	-0.09	-0.47	1.00	0.11	-0.50	1.00	-0.27	-0.46	1.00	-0.23	-0.51	1.00	0.18
x_{opt}	0.05	0.53	1.00	-0.07	0.47	1.00	-0.32	0.18	1.00	-0.38	-0.09	1.00	-0.39	0.11	1.00	-0.19	-0.27	1.00	-0.24	-0.23	1.00	-0.30	0.18	1.00
(2)	$\bar{\mu}$	K_x	K_i	$\bar{\mu}$	K_x	K_i	$\bar{\mu}$	K_x	K_i	$\bar{\mu}$	K_x	K_i	$\bar{\mu}$	K_x	K_i	$\bar{\mu}$	K_x	K_i	$\bar{\mu}$	K_x	K_i	$\bar{\mu}$	K_x	K_i
$\bar{\mu}$	1.00	1.00	-1.00	1.00	1.00	-1.00	1.00	0.99	-0.99	1.00	0.93	-0.95	1.00	0.96	-0.96	1.00	1.00	-1.00	1.00	1.00	-1.00	1.00	1.00	-1.00
K_x	1.00	1.00	-1.00	1.00	1.00	-1.00	0.99	1.00	-0.97	0.93	1.00	-0.86	0.96	1.00	-0.91	1.00	1.00	-1.00	1.00	1.00	-1.00	1.00	1.00	-1.00
K_i	-1.00	-1.00	1.00	-1.00	-1.00	1.00	-0.99	-0.97	1.00	-0.95	-0.86	1.00	-0.96	-0.91	1.00	-1.00	-1.00	1.00	-1.00	-1.00	1.00	-1.00	-1.00	1.00
(3)	a	b	c	a	b	c	a	b	c	a	b	c	a	b	c	a	b	c	a	b	c	a	b	c
a	1.00	-0.95	0.72	1.00	-0.94	0.72	1.00	-0.90	0.62	1.00	-0.87	0.55	1.00	-0.89	0.58	1.00	-0.91	0.69	1.00	-0.90	0.64	1.00	-0.92	0.70
b	-0.95	1.00	-0.85	-0.94	1.00	-0.86	-0.90	1.00	-0.79	-0.87	1.00	-0.72	-0.89	1.00	-0.74	-0.91	1.00	-0.86	-0.90	1.00	-0.83	-0.92	1.00	-0.85
c	0.72	-0.85	1.00	0.72	-0.86	1.00	0.62	-0.79	1.00	0.55	-0.72	1.00	0.58	-0.74	1.00	0.69	-0.86	1.00	0.64	-0.83	1.00	0.70	-0.85	1.00
(4)	$\bar{\mu}$	K_x	K_i	$\bar{\mu}$	K_x	K_i	$\bar{\mu}$	K_x	K_i	$\bar{\mu}$	K_x	K_i	$\bar{\mu}$	K_x	K_i	$\bar{\mu}$	K_x	K_i	$\bar{\mu}$	K_x	K_i	$\bar{\mu}$	K_x	K_i
$\bar{\mu}$		-			-			-		1.00	0.96	-0.97	1.00	0.99	-0.99		-			-			-	
K_x		-			-			-		0.96	1.00	-0.91	0.99	1.00	-0.97		-			-			-	
K_i		-			-			-		-0.97	-0.91	1.00	-0.99	-0.97	1.00		-			-			-	
(5)	$\gamma_{\max}$	$x^\star$		$\gamma_{\max}$	$x^\star$		$\gamma_{\max}$	$x^\star$		$\gamma_{\max}$	$x^\star$		$\gamma_{\max}$	$x^\star$		$\gamma_{\max}$	$x^\star$		$\gamma_{\max}$	$x^\star$		$\gamma_{\max}$	$x^\star$	
$\gamma_{\max}$	1.00	-0.81		1.00	-0.78		1.00	-0.39		1.00	0.07		1.00	-0.18		1.00	-0.05		1.00	-0.14		1.00	-0.48	
$x^\star$	-0.81	1.00		-0.78	1.00		-0.39	1.00		0.07	1.00		-0.18	1.00		-0.05	1.00		-0.14	1.00		-0.48	1.00	

Table 2: Correlation matrix of parameter estimation error of five descriptions (1)-(5) for eight microalgae species (1: *Skeletonema costatum*, 2: *Isochrysis galbana*, 3: *Dunaliella salina*, 4: *Platymonus subcordiformis*, 5: *Chlorococcum sp.* FACHB-1556, 6: *Microcystis aeruginosa* FACHB-905, 7: *Microcystis wesenbergii* FACHB-1112, 8: *Scenedesmus obliquus* FACHB-116). Note that "$-$" represents the case where the Fisher information matrix F is singular, and we cannot obtain an accurate result.

Platymonus subcordiformis and *Chlorococcum sp.* FACHB-1556, where AIC_c and BIC are not able to distinguish. Furthermore, we observe that the description (1) has the minimum value of PEMAC most of the time, except for the species *Platymonus subcordiformis* and *Chlorococcum sp.* FACHB-1556, where the description (5) has the minimum PEMAC value. Otherwise, our description (5) is often the second or the third-best description, meaning that it also provides a good representation of the growth rate with respect to the irradiance using only two parameters. Regarding the description (4), we are only able to provide the PEMAC value for two species, as we need the Fisher information matrix F to compute the average error propagation (20).

3.4. Prediction interval and parameter sensitivity

To further check the quality of using each description μ^k to characterize the growth rate with respect to the irradiance, we show the prediction interval (PI) (15) of each description for all eight microalgae species in Figure A.2-A.9. From the scale and shape of the PI, we observe that the descriptions (1) and (5) provide a relatively good prediction compare with the other three descriptions (2)-(4). And once again, we are only able to show the PI curve of the description (4) for the species *Platymonus subcordiformis* and *Chlorococcum sp.* FACHB-1556, this is due to the singularity of the Fisher information matrix F for the other species.

We can also study the parameter sensitivity using the normalized sensitivity (16). Figures B.10-B.17 present the normalized sensitivity of each description μ^k with respect to the related parameter set θ^k for the eight microalgae species.

For the description (1), we observe that the parameter α (red curve) has a strong sensitivity for small irradiance values, since α represents the initial slope of the growth rate curve. Moreover, $\mu_{\max}$ (blue curve) is the most sensitive parameter when the irradiance approaches to x_{opt}, and the sensitivities of α and x_{opt} (yellow curve) go to zero. This is related to the partial derivatives $\frac{\partial \mu^1}{\partial \theta_j^1}$. Indeed, when x approaches to x_{opt}, the partial derivatives $\frac{\partial \mu^1}{\partial \alpha}$, $\frac{\partial \mu^1}{\partial x_{\text{opt}}}$ are both close to 0 and $\frac{\partial \mu^1}{\partial \mu_{\max}}$ is close to 1. Thus, $\mu_{\max}$ is the most sensitive parameter around x_{opt}. When moving to large values of irradiance, we observe that x_{opt} becomes more sensitive than the other two parameters.

Concerning the descriptions (2) and (4), we observe that the parameter $\bar{\mu}$ (blue curve) is relatively sensitive along with the irradiance, the sensitivity of the parameter K_x (red curve) decreases as the irradiance increases, and the sensitivity of the parameter K_i (yellow curve) increases as the irradiance decreases, which is in line with the structure of this description, where K_x dominates the numerator at low light and x^2/K_i at high light.

	(1)	(2)	(3)	(4)	(5)
Skeletonema costatum					
AIC_c	-561.7971	-561.7971	-561.7971	-554.3161	-557.3357
BIC	-559.7858	-559.7858	-559.7858	-552.3049	-555.3959
PEMAC	-1082.4752	-928.9370	-1028.5730	-	-1060.1172
Isochrysis galbana					
AIC_c	-167.2731	-167.2731	-167.2731	-150.9055	-155.2388
BIC	-170.0133	-170.0133	-170.0133	-153.6457	-156.2106
PEMAC	-333.9981	-211.7551	-302.2497	-	-296.7996
Dunaliella salina					
AIC_c	-168.9626	-168.9626	-168.9626	-160.3860	-164.7193
BIC	-171.7028	-171.7028	-171.7028	-163.1262	-165.6911
PEMAC	-341.5794	-287.4636	-317.7917	-	-329.9519
Platymonus subcordiformis					
AIC_c	-150.1121	-150.1121	-150.1121	-150.1121	-149.3011
BIC	-152.8523	-152.8523	-152.8523	-152.8523	-150.2729
PEMAC	-290.3377	-260.5042	-275.0006	-252.3863	-299.8248
Chlorococcum sp. FACHB-1556					
AIC_c	-168.7907	-168.7907	-168.7907	-168.7907	-171.8261
BIC	-171.5309	-171.5309	-171.5309	-171.5309	-172.7979
PEMAC	-333.2404	-295.6872	-314.1104	-275.4283	-348.9473
Microcystis aeruginosa FACHB-905					
AIC_c	-132.6640	-132.6640	-132.6640	-105.0685	-109.7828
BIC	-136.4387	-136.4387	-136.4387	-108.8432	-111.3281
PEMAC	-259.9892	-157.6629	-236.6074	-	-219.0630
Microcystis wesenbergii FACHB-1112					
AIC_c	-153.6035	-153.6035	-153.6035	-126.5084	-130.8417
BIC	-156.3437	-156.3437	-156.3437	-129.2486	-131.8136
PEMAC	-302.4023	-137.3329	-279.3771	-	-262.9083
Scenedesmus obliquus FACHB-116					
AIC_c	-140.6828	-140.6828	-140.6828	-113.2002	-117.9145
BIC	-144.4574	-144.4574	-144.4574	-116.9749	-119.4598
PEMAC	-278.5561	-177.7300	-252.0564	-	-232.4748

Table 3: The AIC_c, BIC and PEMAC values of the descriptions (1)-(5) for each microalgae species in [27] and [28]

.

For the description (3), we observe that the parameter c (yellow curve) is relatively sensitive only for small irradiance values, the sensitivity of the parameter a (blue curve) increases as the irradiance increases, and the sensitivity curve of the parameter b (red curve) shares the same shape as the growth rate. Recall that the parameter c is related to the initial slope of the growth rate, which explains its sensitivity for small irradiance values.

Regarding our description (5), we observe that the sensitivity curves of the parameters $\gamma_{\max}$ and $x^\star$ are rather symmetric, with a horizontal symmetrical axis at 0.5. Parameter $x^\star$ represents the value for which growth is maximum, and $\gamma_{\max}$ is proportional to the maximum growth rate. The role of both parameters is well-balanced, and they share equally the task of representing the growth rate with respect to the irradiance. Moreover, we find that α in description (1) is only sensitive for small irradiance, $\mu_{\max}$ and x_{opt} rather dominate separately for the rest part. This actually confirms the behavior of our description (5), as $\gamma_{\max}$ and $x^\star$ are much related to $\mu_{\max}$ and x_{opt} respectively. By well choosing these two parameters using (9), our description (5) can very efficiently capture the growth rate.

4. Conclusion

In this study, we have examined four descriptions (1)-(4) of the Haldane model existing in the literature, and introduced an additional description (5) based on only two parameters. The description (4), even if it has been used in the literature, has identifiability problems which lead to disastrous numerical consequences. Descriptions (2) and (3) exhibit strong correlation between parameters and subsequent poor prediction accuracy. The descrition (1), which uncorrelates efficiently the three parameters is the most efficient representation with three parameters. Surprisingly, the two-parameter description (5) out-competes all the other models.

This conclusion on the ability of the description (5) to accurately represent inhibition of photosynthetic organisms by high light would need to be verified with other cases of growth inhibition (Volatile fatty acids, ethanol, phenol, ...). It perfectly illustrates the "Keep It Simple (KIS)" principle, which should guide modelling [29]. With fewer parameters, the identification procedure is more efficient and eventually the modelling uncertainty are better contained than a more complex model, which pay the price of having more parameters.

References

[1] P. Spolaore, C. Joannis-Cassan, E. Duran, and A. Isambert. Commercial applications of microalgae. *Journal of Bioscience and Bioengineering*, 101(2):87–96, 2006.

[2] E.W. Becker. Micro-algae as a source of protein. *Biotechnology Advances*, 25(2):207–210, 2007.

[3] Y. Wang, S.M. Tibbetts, and P.J. McGinn. Microalgae as sources of high-quality protein for human food and protein supplements. *Foods*, 10(12), 2021.

[4] S.-Y. Lee and H.-U. Kim. Systems strategies for developing industrial microbial strains. *Nature Biotechnology*, 33(10):1061–1072, 2015.

[5] S. Jagadevan, A. Banerjee, C. Banerjee, C. Guria, R. Tiwari, M. Baweja, and P. Shukla. Recent developments in synthetic biology and metabolic engineering in microalgae towards biofuel production. *Biotechnol Biofuels*, (11), 2018.

[6] T.M. Mata, A.A. Martins, and N.S. Caetano. Microalgae for biodiesel production and other applications: A review. *Renewable and Sustainable Energy Reviews*, 14(1):217–232, 2010.

[7] H. Narayanan, M. F. Luna, M. von Stosch, M. N. Cruz Bournazou, G. Polotti, M. Morbidelli, A. Butté, and M. Sokolov. Bioprocessing in the digital age: the role of process models. *Biotechnology journal*, 15(1):1900172, 2020.

[8] J. Monod. *Recherches sur la Croissance des Cultures Bactériennes.* Hermann, Paris, 1942.

[9] S. Aiba, M. Shoda, and M. Nagatani. Kinetics of product inhibition in alcohol fermentation. *Biotechnology and Bioengineering*, 10(6):845–864, 1968.

[10] V.H. Edwards. The influence of high substrate concentrations on microbial kinetics. *Biotechnology and Bioengineering*, 12(5):679–712, 1970.

[11] M. Muloiwa, S. Nyende-Byakika, and M. Dinka. Comparison of unstructured kinetic bacterial growth models. *South African Journal of Chemical Engineering*, 33:141–150, 2020.

[12] J.B.S. Haldane. *Enzymes.* Cambridge, Cambridge, 1965.

[13] E.A. Seagren, H. Kim, and B.F. Smets. Identifiability and retrievability of unique parameters describing intrinsic Andrews kinetics. *Applied Microbiology and Biotechnology*, 61(4):314–322, 2003.

[14] W.-D. Liu and C.-Y. Lee. Practical identification analysis of Haldane kinetic parameters describing phenol biodegradation in batch operations. Journal of Environmental Engineering and Management, 2007.

[15] O. Bernard and B. Rémond. Validation of a simple model accounting for light and temperature effect on microalgal growth. *Bioresource Technology*, 123:520–527., 2012.

[16] H. Taher, S. Al-Zuhair, A. Al-Marzouqi, Y. Haik, and M. Farid. Growth of microalgae using CO_2 enriched air for biodiesel production in supercritical CO_2. *Renewable Energy*, 82:61–70, 2015.

[17] A. Banerjee and A. K. Ghoshal. Phenol degradation by Bacillus cereus: pathway and kinetic modeling. *Bioresource Technology*, 101(14):5501–5507, 2010.

[18] C. García-Diéguez, O. Bernard, and E. Roca. Reducing the Anaerobic digestion model No. 1 for its application to an industrial wastewater treatment plant treating winery effluent wastewater. *Bioresource technology*, 132:244–253, 2013.

[19] O Bernard and L.-D. Lu. Optimal optical conditions for microalgal production in photobioreactors. *Journal of Process Control*, 112:69–77, 2022.

[20] J.F. Andrews. A mathematical model for the continuous culture of microorganisms utilizing inhibitory substrates. *Biotechnology and Bioengineering*, 10(6):707–723, 1968.

[21] J.C.H. Peeters and P. Eilers. The relationship between light intensity and photosynthesis—A simple mathematical model. *Hydrobiological Bulletin*, 12(2):134–136, 1978.

[22] P.B. Kenneth and R.A. David, editors. *Model Selection and Multimodel Inference.* Springer-Verlag New York, 1998.

[23] K.P. Burnham, D.R. Anderson, and Huyvaert K.P. AIC model selection and multimodel inference in behavioral ecology: some background, observations, and comparisons. *Behavioral ecology and sociobiology*, 65(1):23–35, 2011.

[24] G. James, D. Witten, T. Hastie, and R. Tibshirani. *An introduction to statistical learning.* Springer, 2013.

[25] A.D.R McQuarrie and C.-L. Tsai. *Regression and Time Series Model Selection.* WORLD SCIENTIFIC, 1998.

[26] K.P. Burnham and D. R. Anderson. Multimodel inference: Understanding AIC and BIC in model selection. *Sociological Methods and Research*, 33(2):261–304, 2004.

[27] T. Anning, H.L. MacIntyre, S.M. Pratt, P.J. Sammes, S. Gibb, and R.J. Geider. Photoacclimation in the marine diatom Skeletonema costatum. *Limnology and Oceanography*, 45(8):1807–1817, 2000.

[28] X.L. Yang, L.H. Liu, Z.K. Yin, X.Y Wang, S.B Wang, and Z.P. Ye. Quantifying photosynthetic performance of phytoplankton based on photosynthesis–irradiance response models. *Environmental sciences Europe*, 32(1), 2020.

[29] F. Mairet and O. Bernard. Twelve quick tips for designing sound dynamical models for bioprocesses. *PLoS Computational Biology*, 15(8):e1007222, 2019.

[30] S. Chatterjee and A.S. Hadi. *Regression Analysis by Example.* Wiley Series in Probability and Statistics. Wiley, 2006.

[31] J. C. Lagarias, J. A. Reeds, M. H. Wright, and P. E. Wright. Convergence properties of the Nelder–Mead simplex method in low dimensions. *SIAM Journal on optimization*, 9(1):112–147, 1998.

[32] J.F. van Impe, P.A. Vanrolleghem, and D.M. Iserentant, editors. *Advanced Instrumentation, Data Interpretation, and Control of Biotechnological Processes*. Springer Netherlands, 1998.

[33] F. Casagli, S. Rossi, J. P. Steyer, O. Bernard, and E. Ficara. Balancing microalgae and nitrifiers for wastewater treatment: can inorganic carbon limitation cause an environmental threat? *Environmental science & technology*, 55(6):3940–3955, 2021.

[34] J. Cariboni, D. Gatelli, R. Liska, and A. Saltelli. The role of sensitivity analysis in ecological modelling. *Ecological Modelling*, 203(1):167–182, 2007. Special Issue on Ecological Informatics: Biologically-Inspired Machine Learning.

Appendix A. Prediction intervals

We present the prediction intervals of the five descriptions (1)-(5) for each microalgae specie. For all figures, the blue points represent the experimental data obtained from [27, 28], the red line is the fitted curve using the optimal parameter values obtained in Table 1. The purple (resp. yellow) dashed line is the upper (resp. lower) bound of the prediction interval computed using (15). Note that we can only find prediction intervals for four description in some tested cases, as the Fisher information matrix for the description (4) is singular. Hence, we cannot compute e in (15) in these cases. Recall also that Z is the value in the two-tailed Student's t-table. For the experimental data in [27, 28], when the size of samples n is 12, $Z = 2.201$, $Z = 2.179$ when $n = 13$, and $Z = 2.080$ when $n = 22$.

Skeletonema costatum

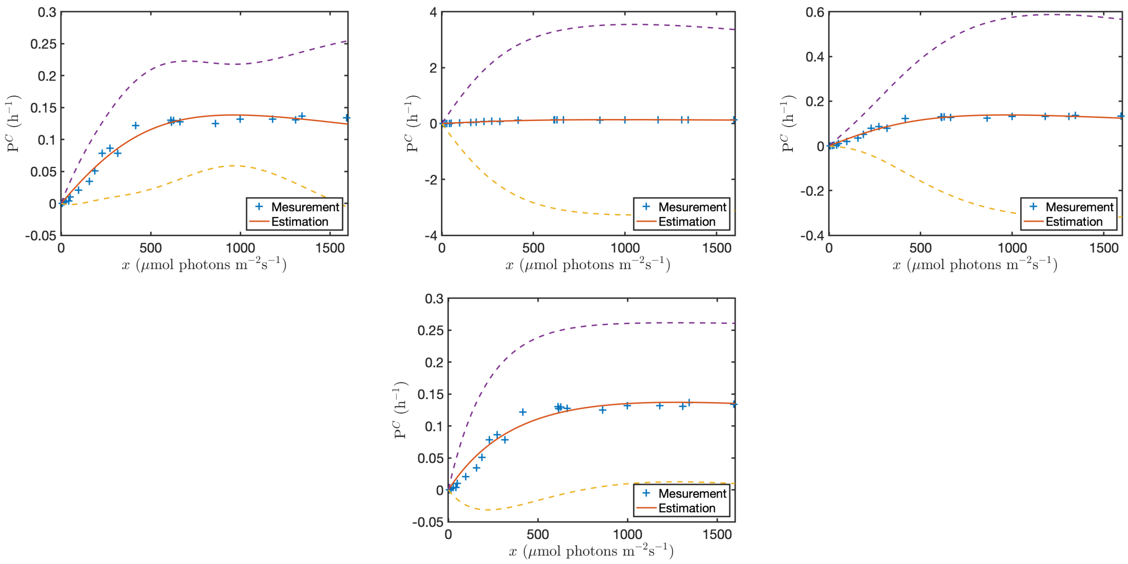

Figure A.2: Prediction intervals of four descriptions (1)-(3) and (5) with respect to the irradiance x for the experimental data of *Skeletonema costatum* [27]. Top left: (1). Top middle: (2). Top right: (3). Bottom: (5).

Isochrysis galbana

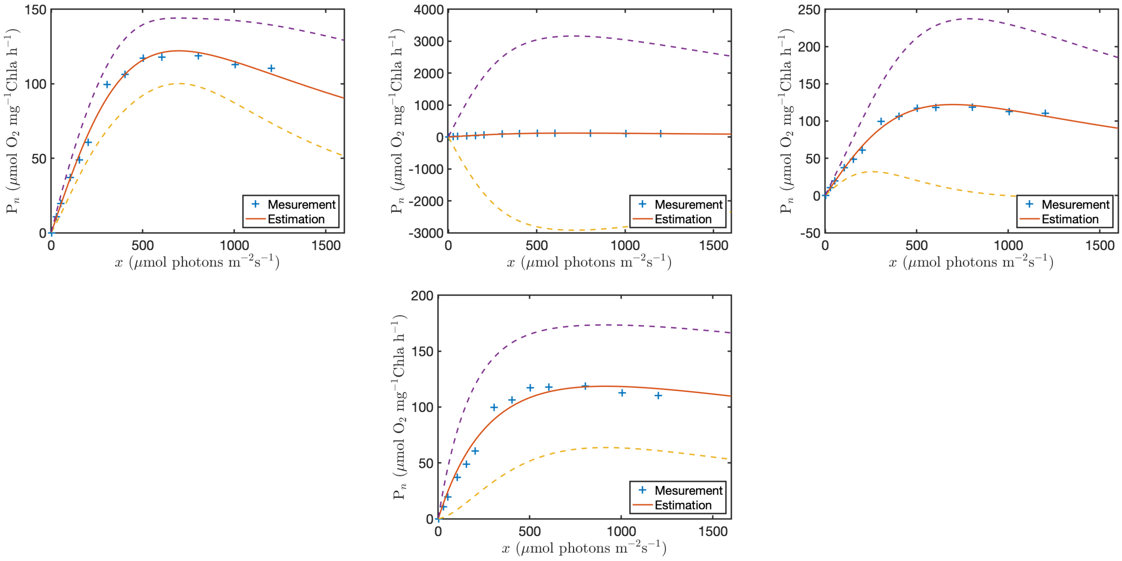

Figure A.3: Prediction intervals of four descriptions (1)-(3) and (5) with respect to the irradiance x for the experimental data of *Isochrysis galbana* [28]. Top left: (1). Top middle: (2). Top right: (3). Bottom: (5).

.

Dunaliella salina

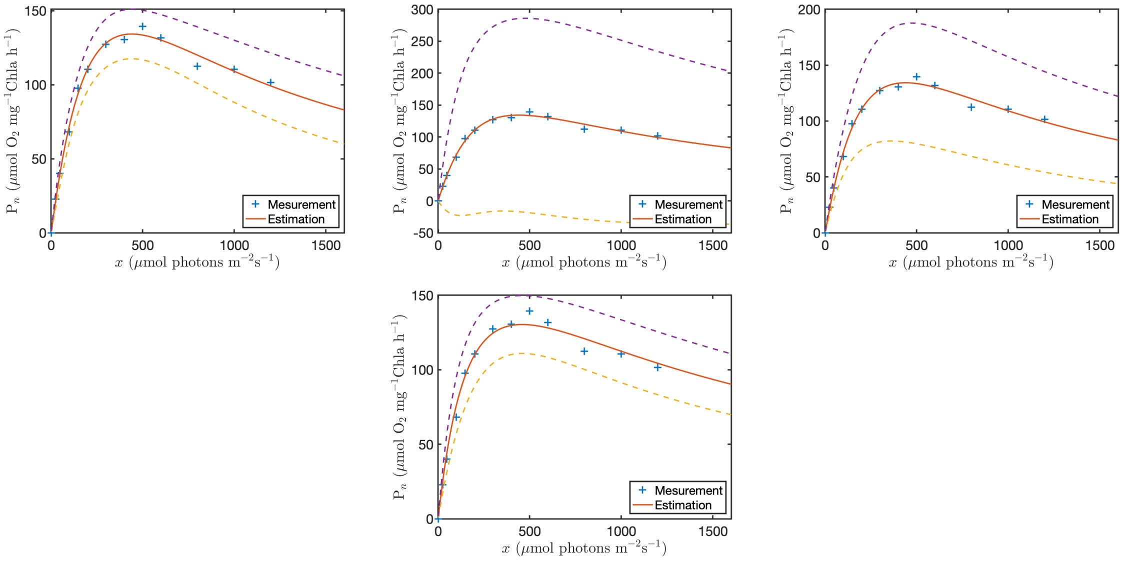

Figure A.4: Prediction intervals of four descriptions (1)-(3) and (5) with respect to the irradiance x for the experimental data of *Dunaliella salina* [28]. Top left: (1). Top middle: (2). Top right: (3). Bottom: (5).

Platymonus subcordiformis

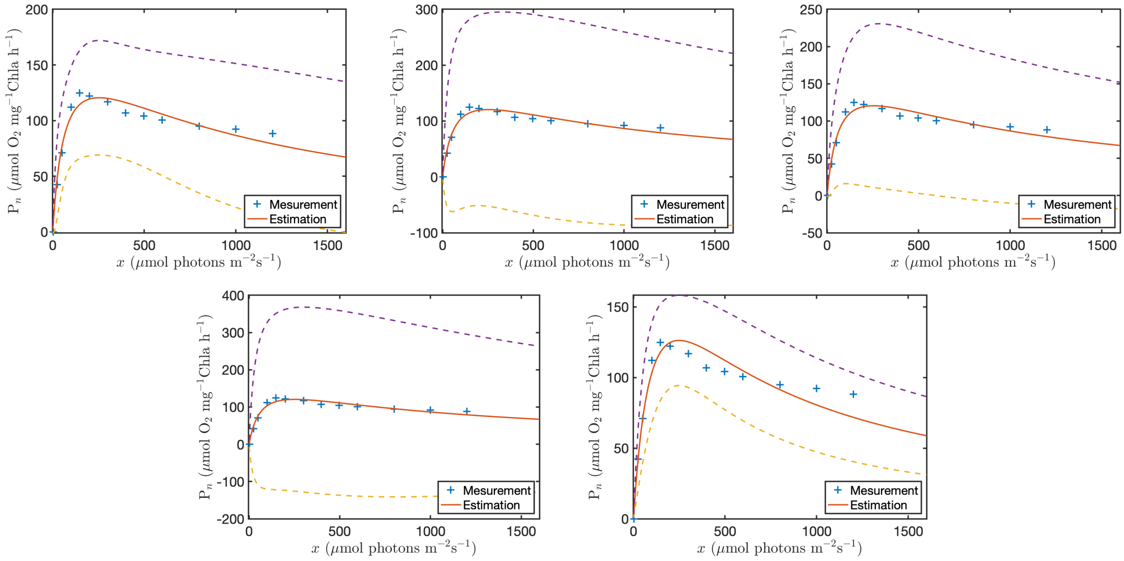

Figure A.5: Prediction intervals of five descriptions (1)-(5) with respect to the irradiance x for the experimental data of *Platymonus subcordiformis* [28]. Top left: (1). Top middle: (2). Top right: (3). Bottom left: (4). Bottom right: (5).

Chlorococcum sp. FACHB-1556

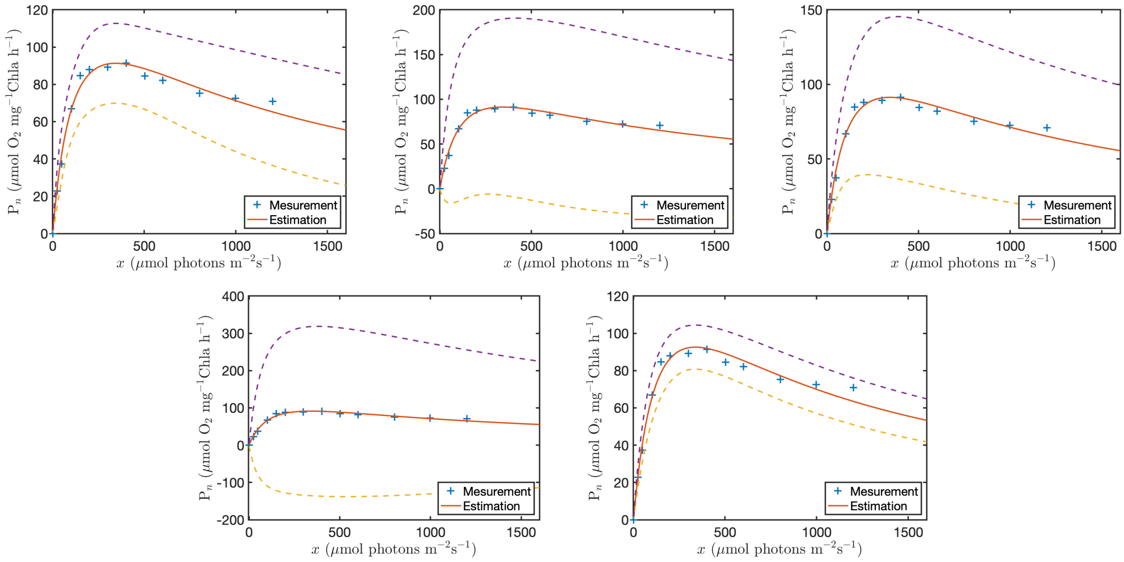

Figure A.6: Prediction intervals of five descriptions (1)-(5) with respect to the irradiance for the experimental data of *Chlorococcum sp.* FACHB-1556 [28]. Top left: (1). Top middle: (2). Top right: (3). Bottom left: (4). Bottom right: (5).

Microcystis aeruginosa FACHB-905

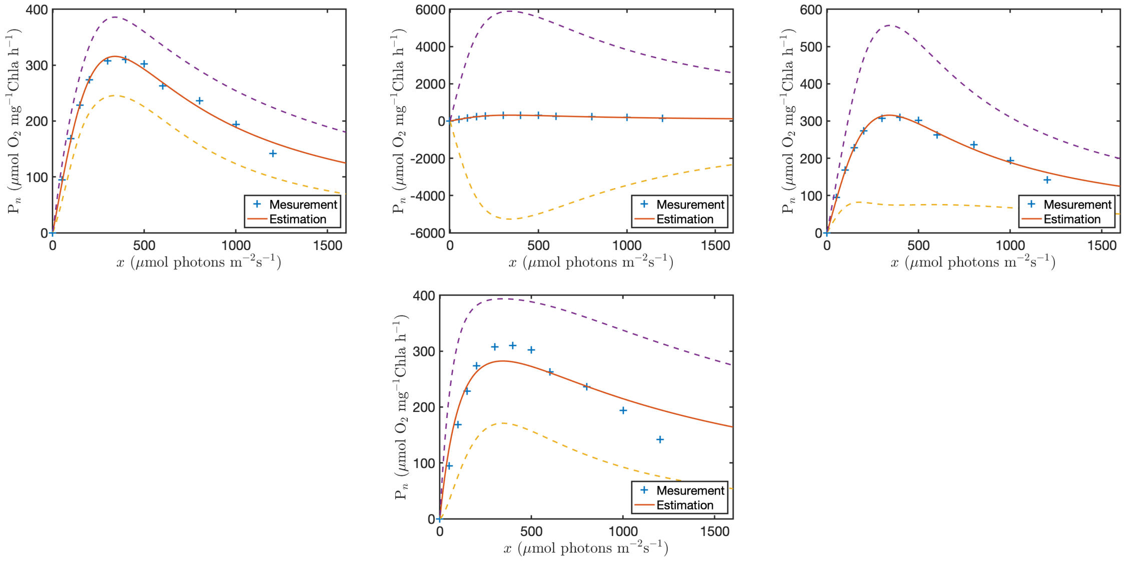

Figure A.7: Prediction intervals of four descriptions (1)-(3) and (5) with respect to the irradiance x for the experimental data of *Microcystis aeruginosa* FACHB-905 [28]. Top left: (1). Top middle: (2). Top right: (3). Bottom: (5).

Microcystis wesenbergii FACHB-1112

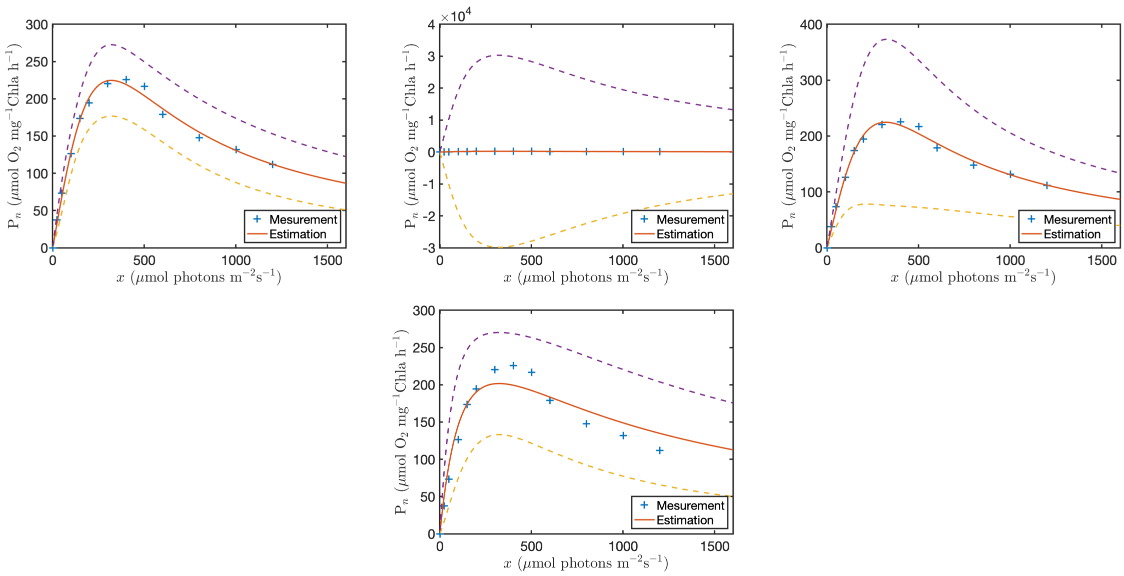

Figure A.8: Prediction intervals of four descriptions (1)-(3) and (5) with respect to the irradiance x for the experimental data of *Microcystis wesenbergii* FACHB-1112 [28]. Top left: (1). Top middle: (2). Top right: (3). Bottom: (5).

Scenedesmus obliquus FACHB-116

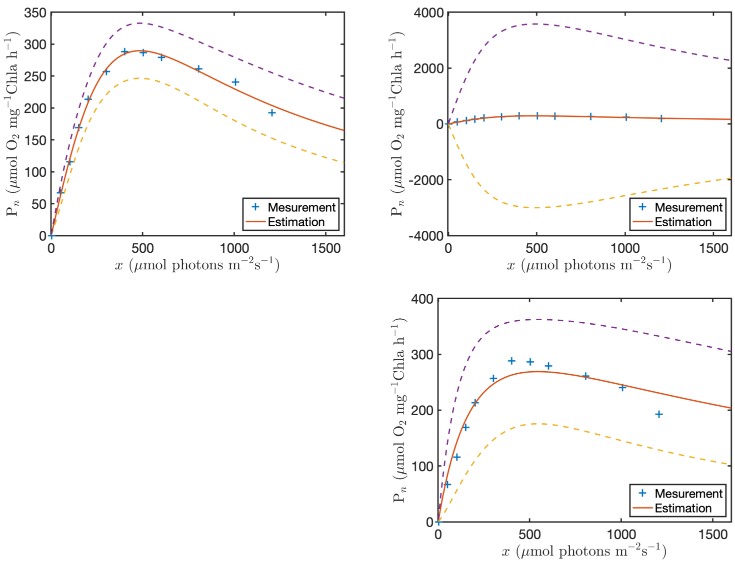

Figure A.9: Prediction intervals of four descriptions (1)-(3) and (5) with respect to the irradiance x for the experimental data of *Scenedesmus obliquus* FACHB-116 [28], Top left: (1). Top middle: (2). Top right: (3). Bottom: (5).

Appendix B. Normalized sensitivity

We present here the normalized sensitivity of all five descriptions (1)-(5) for each microalgae specie using (16). Once again, we cannot present the results of the description (4) in some cases, as the Fisher information matrix is singular.

Skeletonema costatum

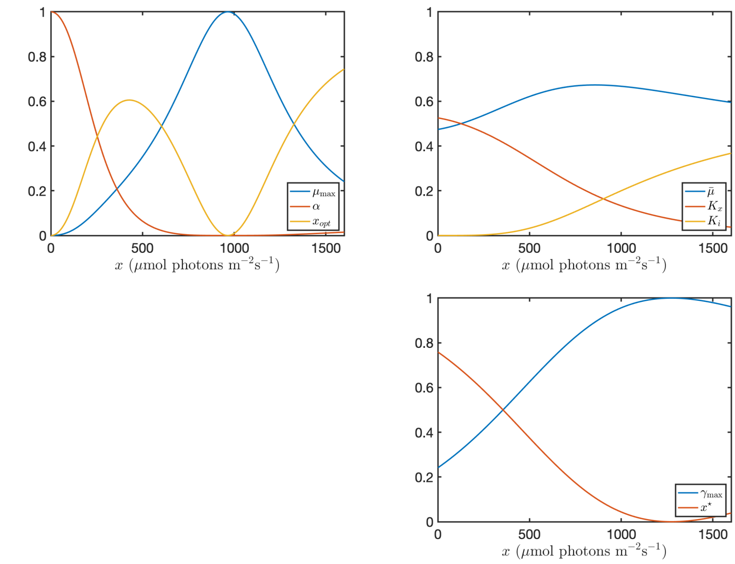

Figure B.10: Normalized sensitivity for each parameter of four descriptions (1)-(3) and (5) with respect to the irradiance x for the experimental data of *Skeletonema costatum* [27]. Top left: (1). Top middle: (2). Top right: (3). Bottom: (5).

Isochrysis galbana

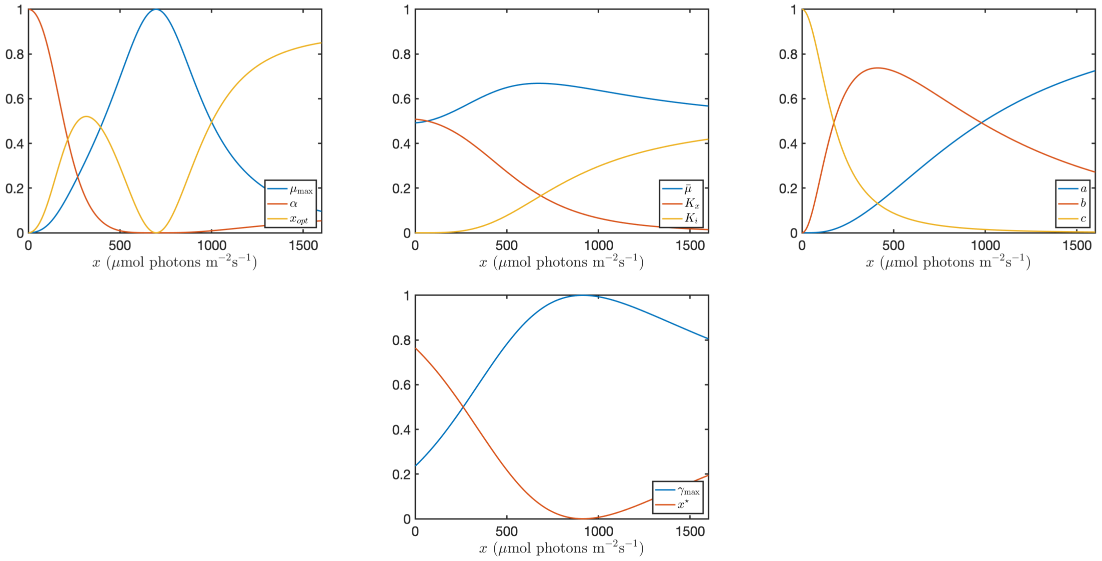

Figure B.11: Normalized sensitivity for each parameter of four descriptions (1)-(3) and (5) with respect to the irradiance x for the experimental data of *Isochrysis galbana* [28]. Top left: (1). Top middle: (2). Top right: (3). Bottom: (5).

Dunaliella salina

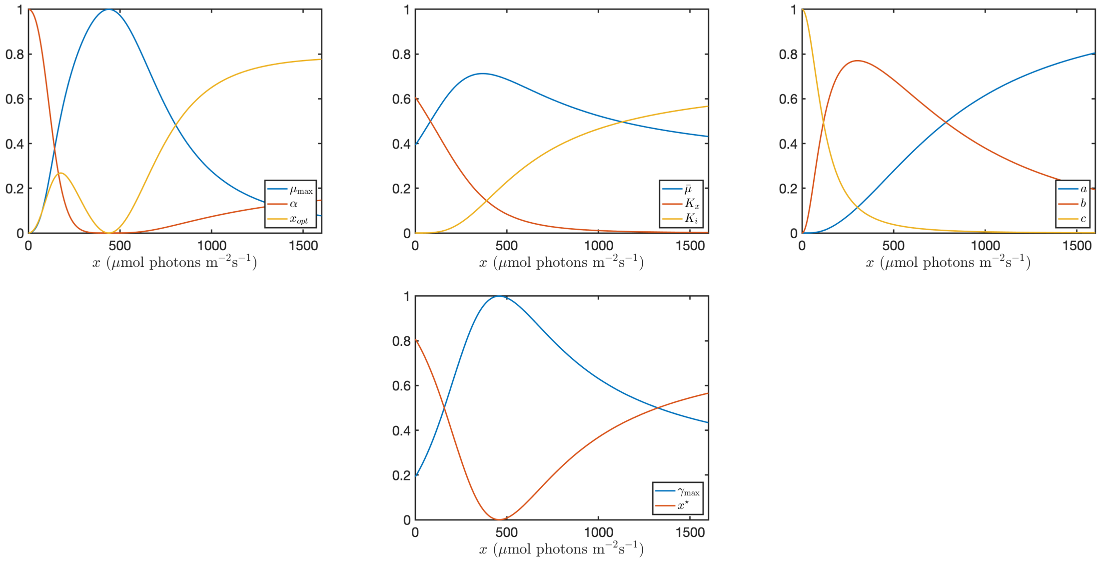

Figure B.12: Normalized sensitivity for each parameter of four descriptions (1)-(3) and (5) with respect to the irradiance x for the experimental data of *Dunaliella salina* [28]. Top left: (1). Top middle: (2). Top right: (3). Bottom: (5).

Platymonus subcordiformis

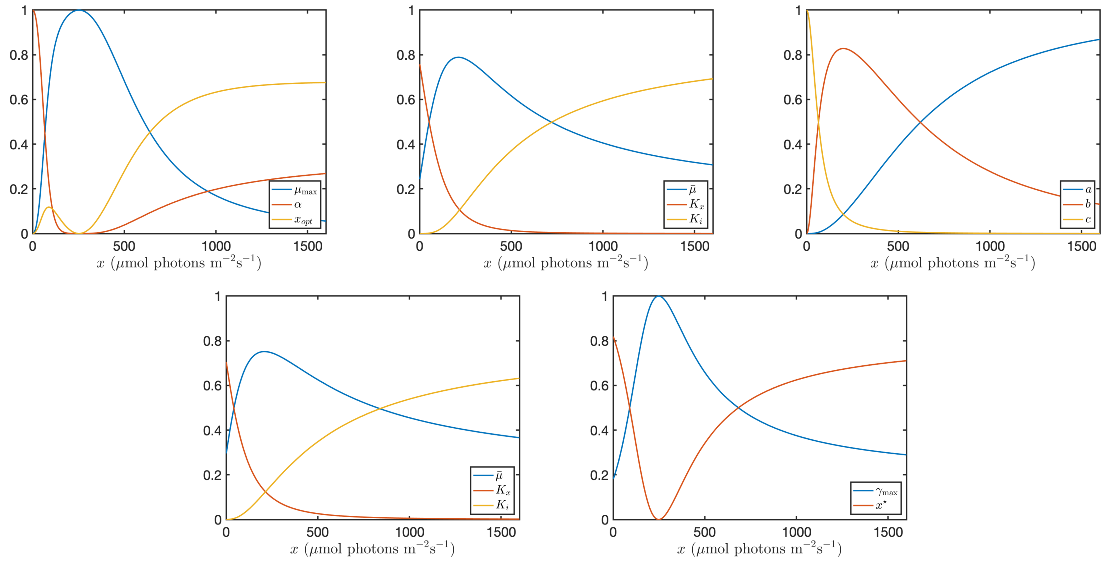

Figure B.13: Normalized sensitivity for each parameter of five descriptions (1)-(5) with respect to the irradiance x for the experimental data of *Platymonus subcordiformis* [28]. Top left: (1). Top middle: (2). Top right: (3). Bottom left: (4). Bottom right: (5).

Chlorococcum sp. FACHB-1556

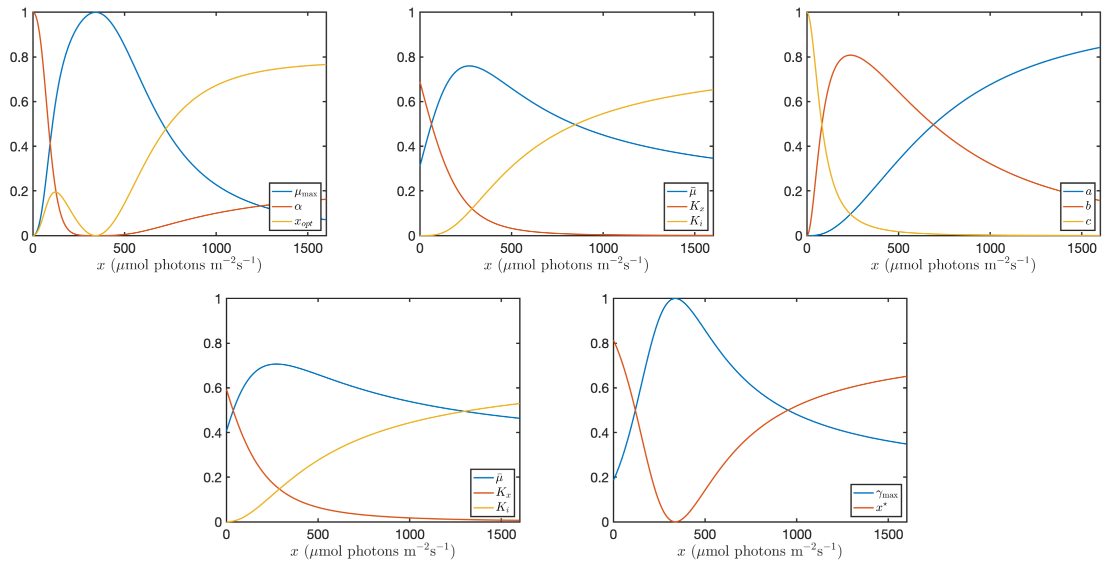

Figure B.14: Normalized sensitivity for each parameter of five descriptions (1)-(5) with respect to the irradiance x for the experimental data of *Chlorococcum sp.* FACHB-1556 [28]. Top left: (1). Top middle: (2). Top right: (3). Bottom left: (4). Bottom right: (5).

Microcystis aeruginosa FACHB-905

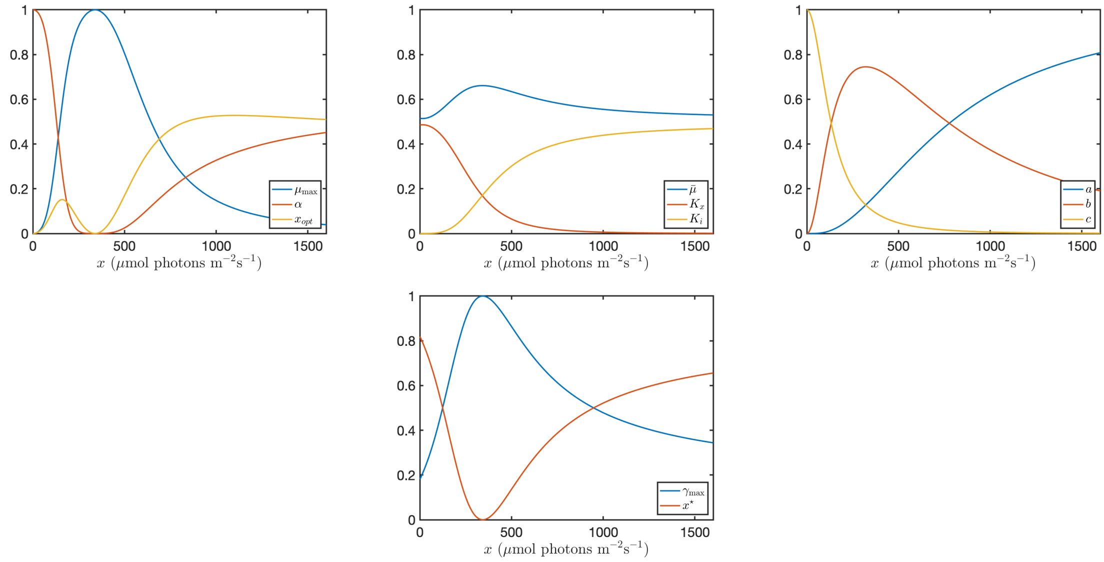

Figure B.15: Normalized sensitivity for each parameter of four descriptions (1)-(3) and (5) with respect to the irradiance x for the experimental data of *Microcystis aeruginosa* FACHB-905 [28]. Top left: (1). Top middle: (2). Top right: (3). Bottom: (5).

Microcystis wesenbergii FACHB-1112

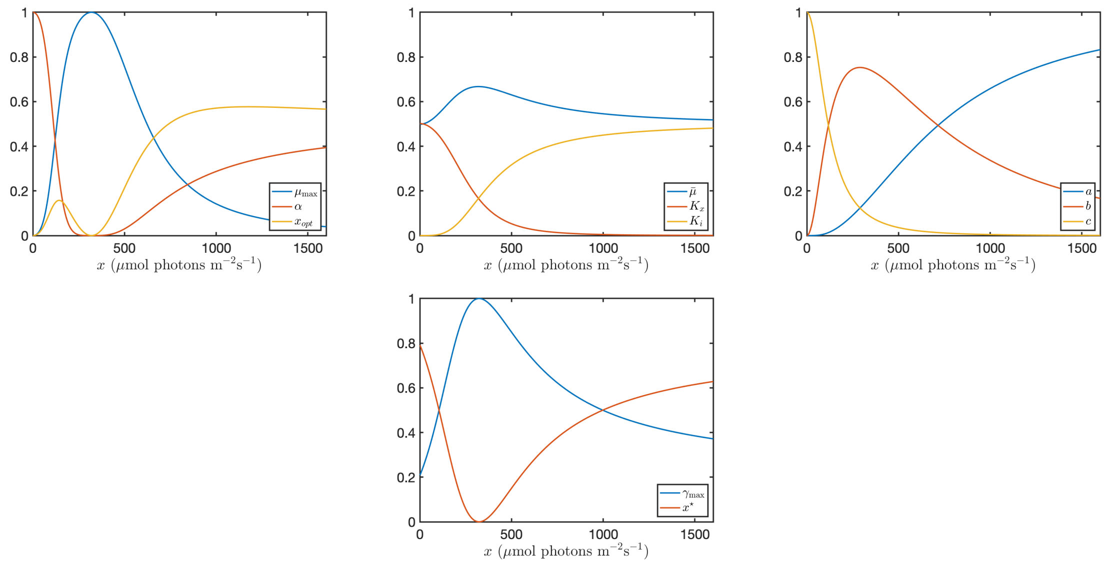

Figure B.16: Normalized sensitivity for each parameter of four descriptions (1)-(3) and (5) with respect to the irradiance x for the experimental data of *Microcystis wesenbergii* FACHB-1112 [28].Top left: (1). Top middle: (2). Top right: (3). Bottom: (5).

Scenedesmus obliquus FACHB-116

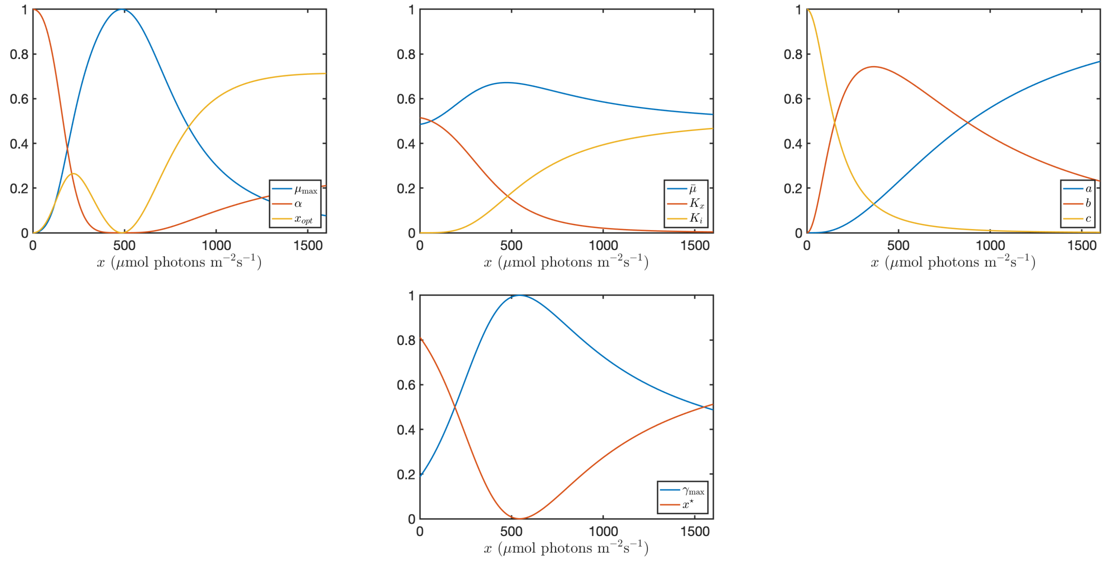

Figure B.17: Normalized sensitivity for each parameter of four descriptions (1)-(3) and (5) with respect to the irradiance x for the experimental data of *Scenedesmus obliquus* FACHB-116 [28]. Top left: (1). Top middle: (2). Top right: (3). Bottom: (5).